

## High Temperature Superconducting (HTS) Generator Field Coil System Fault Analysis

David I Eromon, Ph.D, Assistant Professor, Department of Electronics, Computer and Information Technology, North Carolina A&T State University, USA; [dieromon@ncat.edu](mailto:dieromon@ncat.edu)

P. A. Edigin, BDPA Energy Commission, Nigeria

### Abstract

Coils with high temperature superconducting (HTS) are generally stable against transient thermal disturbances. Protection against spontaneous quenches is not a main design issue for an HTS coil Sivasubramaniam, K, *et al.* However HTS coils used in many electric devices such as motors, generators, transformers, and current limiters will operate under over-current fault conditions, which may result in a coil quench and thermal runaway. Those electric devices should be able to ride through some grid fault conditions and remain functional. This requires a certain over-current capability of the HTS coils. This paper discusses the over-current requirements from grid faults and the thermal transient responses of a Bismuth Strontium Calcium Copper Oxide (BSCCO) coil.

### List of Symbols

$P_{tot}$  - The total losses

FE - Finite-element

$t_{per}$  - The period time

$(W m^{-1})$  - The flux-flow losses per unit length

$P_{strip}$  - The hysteresis losses due to the perpendicular component of the self-field

$P_{fff}$  - Sum of the flux-flow losses

$P_{slab}$  - The hysteresis losses in a slab due to the combined action of a parallel magnetic field and a transport current

$t_{per}$  - The period time

$E_{dc}$  - is the electric field

$I$  - is the current

$I_c$  - Critical current criterion

$f$  - is the frequency

$CA$  - an effective area

$B_p$  - the penetration field

$\beta = B_{peak}/B_p$

$i = I_{peak}/I_c$

$I_F$  = Field current

$\rho_s$  = HTS tape residual resistivity

$\rho_e$  = total conductor resistivity

$A$  = total conductor cross-sectional area

### LIST OF ABBREVIATIONS

HTS - High Temperature Superconducting

DC - Direct Current

BSCCO - Bismuth Strontium Calcium Copper Oxide

### Introduction

The development of high-temperature superconducting (HTS) tapes has advanced to a point where commercial applications may be considered. Long-length, robust BSCCO/Ag tapes with high current

densities are available today on the market [1, 2]. Although manufactured primarily for DC purposes, such tapes have been used in demonstrator projects of e.g., power transmission cables [3–5] and power transformers [6] where the HTS components have been installed in power networks, N Magnusson *et al.* In several applications, e.g., transformers and induction heaters [7], the AC loss is a crucial factor in determining the economical feasibility. The AC losses in the DC HTS tapes currently available are generally too high and an AC HTS tape with reduced AC losses is needed to make many of the power applications commercially attractive. Recent work has led to reliable methods for measuring the AC losses in HTS tapes under application-like conditions [8–11]. From the experimental results, semi-empirical models based on the critical state model [12] have been developed for the AC losses [13–16]. Using these models, the AC losses in a complete HTS component can be predicted with an acceptable accuracy.

Higher operating temperature of high-temperature superconductors (HTS) devices results in a large stability margin for the HTS coil, making spontaneous quenches caused by thermal disturbances very unlikely [22]. Electrical apparatus for power applications are, however, routinely expected to go through transient fault conditions that can result in significant over currents compared with steady-state operation [23], [24]. Such transients are rare and short lived, but may result in a coil quench and thermal runaway. Designing the superconducting coils with enough margin to ride through the over-currents without going normal is not always economically feasible. One approach to the problem is to design the HTS coils to go normal and return to the superconducting state after an over-current event. The design and analysis of the field coil of an HTS synchronous generator being studied by GE following this approach is briefly described in this paper. IEEE and ANSI standards [25] give generic specifications for the required short-term current-carrying capability of the field coil (Table I).

TABLE 1: ANSI C50.15 THERMAL STABILITY REQUIREMENTS

Field current, pu	2.08	1.46	1.25	1.12
Required time (s)	10	30	60	120

The highly nonlinear resistive behavior of the HTS coil during quench requires a more rigorous analysis to qualify the coil for operation under various fault scenarios, including the strong coupling between the EM and thermal conditions and the behavior of the whole electromechanical system. The over-current capability is evaluated by computing the coil currents during a severe fault condition and calculating the resulting coil temperatures. The fault chosen for the analysis is a three-phase sudden short circuit at the high side of the transformer up to the critical fault clearing time of 18 cycles and the subsequent recovery. The temperatures are predicted using an ANSYS FE (finite-element)-based quench model [26]. The FE model includes the HTS coil assembly (coil, heat exchangers, cryogen circuit, coil support structure, and joule heating of the wire splices) and heat transfer through radiation and conduction to the rest of the system. To meet the over-current requirement, the coil must be superconducting at the end of the over-current situation (when it returns to the operating current). In other words, the coil should be equal to or below the current sharing temperature, at the operating current.

### AC Losses Calculation

This paper focuses on the AC losses due the combined effect of transport currents and magnetic fields oriented parallel to the surface of the tape, as is the situation in a large part of a coil. At the ends of a coil the magnetic field contains a component perpendicular to the surface of the tape. Although the losses in this part of the coil are of importance, they are left out of the present discussion since their magnitude very much depends on the design of the coil and the use of magnetic flux diverters. The equations describing the AC losses have been reported in detail elsewhere [14] and will only be briefly reviewed. The model assumes that all current flows within the HTS filaments. For HTS tapes, current sharing between the HTS filaments and the metal matrix occurs at high currents. However, for the considered HTS tape and application, the current carried by the metal matrix is

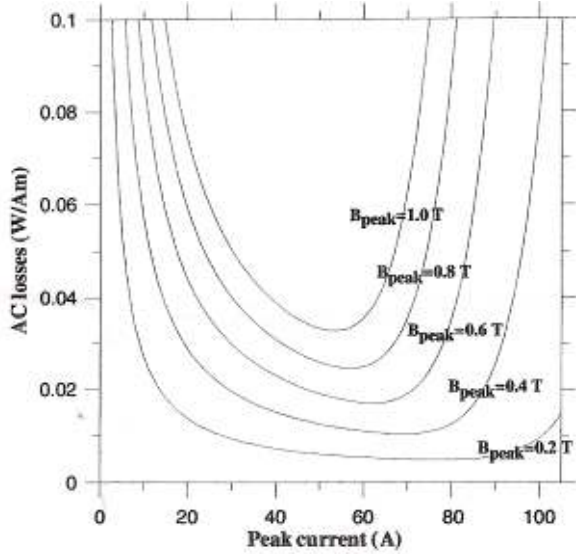


Figure 1: Calculated AC losses per unit carried peak current and unit length as a function of carried current at 80K.

negligible in the interesting region of currents. The total losses,  $P_{tot}$ , are modelled as a sum of the flux-flow losses,  $P_{ff}$ , the hysteresis losses in a slab due to the combined action of a parallel magnetic field and a transport current,  $P_{slab}$ , and the hysteresis losses due to the perpendicular component of the self-field,  $P_{strip}$ ,

$$\text{Type equation here. } P_{tot} = P_{ff} + P_{slab} + P_{strip}. \text{ ----- (1)}$$

The flux-flow losses per unit length ( $W m^{-1}$ ) are given by the equation,

$$P_{ff} = \frac{1}{t_{per}} \int_0^{t_{per}} I E_{dc} dt \text{ -----2}$$

where  $t_{per}$  is the period time,  $I$  is the current and  $E_{dc}$  is the electric field which is given by a power law dependency,

$$E_{dc} = a \left( \frac{I}{I_c(T, B)} \right)^{n(T, B)} \text{ -----3}$$

where  $a$  is  $1 \mu V cm^{-1}$  determined by the chosen standard critical current criterion.  $I_c$  and the exponent  $n$  are fitted to experimental data obtained from DC  $I-E$  measurements. The hysteresis losses per unit length ( $Wm^{-1}$ ) in a slab for currents below  $I_c$  are given by [19],

$$P_{slab} = \begin{cases} \frac{fCAB_p^2}{3\mu_0} [(\beta + i)^3 + (\beta - i)^3] & i < \beta < 1 \\ \frac{fCAB_p^2}{3\mu_0} \left[ 2\beta(3 + i^2) - 4(1 - i^3) + 12i^2 \frac{(1-i)^2}{\beta - i} - 8i^2 \frac{(1-i)^3}{(\beta - i)^2} \right] & 1 < i < \beta \end{cases}$$

$$\frac{fCAB_p^2}{3\mu_0} [(i + \beta)^3 + (i - \beta)^3] \quad \beta < i < 1 \quad \text{-----} \quad 4$$

and for currents above  $I_c$  by [20],

$$P_{\text{slab}} = \begin{cases} \frac{fCAB_p^2}{3\mu_0} \left[ 8 \frac{\beta}{i} \right] & 1 < i < \beta \\ \frac{fCAB_p^2}{3\mu_0} \left( \frac{1}{i} \right)^3 [(i + \beta)^3 + (i - \beta)^3] & \beta < i, i > 1 \quad \text{-----} \quad 5 \end{cases}$$

where  $f$  is the frequency,  $CA$  an effective area,  $B_p$  the penetration field,  $\beta = B_{\text{peak}}/B_p$  and  $i = I_{\text{peak}}/I_c$ .  $CA$  and  $B_p$  are fitting parameters determined from measured values of the AC losses due to magnetic fields at one temperature. The temperature dependency of  $B_p$  is obtained from its linear relationship with the critical current. The  $I_c$  used is the self field critical current. The hysteresis losses per unit length ( $W m^{-1}$ ) due to the self-field component perpendicular to the surface of the tape are for currents below  $I_c$  given by [21],

$$P_{\text{strip}} = \frac{fI_c^2 \mu_0}{\pi} \text{Type equation here.} [(1 - i) \ln(1 - i) + (1 + i) \ln(1 + i) - i^2] \quad i < 1 \quad \text{-----} \quad (6)$$

and for currents above  $I_c$  by [14],

$$P_{\text{strip}} = \frac{fI_c^2 \mu_0}{\pi} [2 \ln 2 - 1] \quad i > 1 \quad \text{-----} \quad 7$$

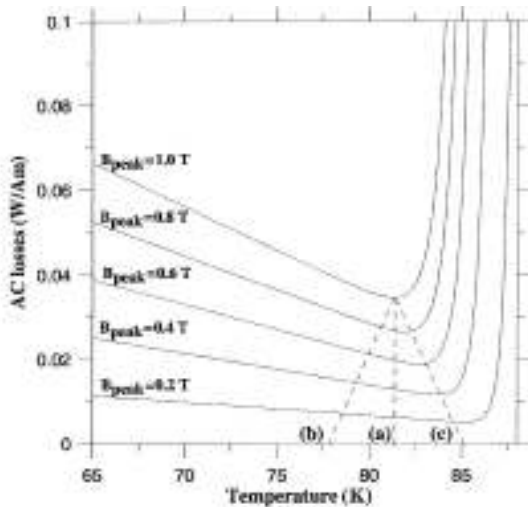


**Figure 2: Calculated AC losses per unit carried peak current and unit length as a function of temperature.**

where again the  $I_c$  used is the self-field critical current. Loss results are given for a multi-filamentary, non-twisted, Bi-2223/Ag HTS tape manufactured by American Superconductor Corporation. The cross section of the tape is 0.21 mm times 4.29 mm and the self-field critical current at 77 K, determined by the  $1 \mu V cm^{-1}$  criterion, is 115 A. The parameter  $CA$  in (4) and (5) is  $0.68 mm^2$ , and the parameter  $B_p$  is 33 mT at 77 K. In figure 1 the AC losses per unit length and unit carried current are given as a function of current for different applied magnetic fields, while figure 2 shows the AC losses per unit length and unit carried current as a function of temperature at different magnetic fields and at a constant current of 44 A. These

graphs constitute the basis for the discussion on AC losses and design optimisation of an HTS coil in the following sections. The AC currents and AC magnetic fields are given in peak values.

### Generator/HTS Coil Design

A study has been conducted by GE on a large HTS generator for power generation. It consists of a conventional stator and a high-temperature superconducting rotor. The high-level parameters of a 100 MVA generator based on this concept are summarized and compared with a conventional generator in Table II. The superconducting rotor coil is a layer-wound racetrack coil using the BSCCO conductor. The conductor contains materials of BSCCO, silver, Pb-Sn solder and stainless steel, and is wrapped with insulation. An extra  $-0.076\text{mm}$  thick prepreg is placed between layers to enhance the layer-to-layer electric insulation. The coil is cooled by a circulating helium gas in a Cu tube placed on the outer surface of the coil. It is surrounded by thin Cu sheets to shield the coil from radiation heat loads and to provide better heat conduction for the coil.

Unlike low-temperature superconductors, a high-temperature superconductor is very stable against thermal disturbances due to its higher heat capacity. The likely quench cause is the operating current's exceeding the critical current, which can be caused by the over-current during a fault event, as discussed in the preceding sections.

**TABLE II: Comparisons of Generator Parameters**

Parameter	100 MVA HTS Generator	Conventional 100 MVA Generator
Rating (MVA)	111.9	111.9
Armature Voltage (kV)	13.8	13.8
Active Length (in)	128	128
Rotor OD (forging)	35.5	37.2
Shield	Aluminum	None
Inertia (sec)	6.66	6.92
No-load Current (A)	39	293
Full-load Current (A)	86.6	833
SCR	0.80	0.48
$X_d$ (pu)	1.46	2.24
$X'd_v$ (pu)	0.36	0.26
$X''_d$ (pu)	0.15	0.15
$T'd_0$ (sec)	4815	8.48
$T''_d_0$ (sec)	0.29	0.04
$Ta_2$ (sec)	0.41	0.38
$X_q$ (pu)	0.92	2.14
$X'q$ (pu)	0.91	0.48
$X''q$ (pu)	0.15	0.15
$T'q_0$ (sec)	32	0.58
$T''q_0$ (sec)	0.82	0.08

When there is a transformer high side fault, the generator is required to stay on line, ride through the fault, and be able to take full rated field current when the fault is cleared. One way for the field coil to have this capability is to have enough current margin so that it stays superconducting even at the peak current during a fault. But this would require much more superconductor than otherwise needed. Note that the peak current can be 2 to 3 times higher than the normal operating current, and that as the current increases, so does the local peak field, which reduces significantly the HTS critical current. To make the coil more cost effective, we should allow the over-current to exceed the coil during a fault if the coil temperature stays low enough to accept the full operating current at the end of the fault. This more cost-effective Fig. 4, System model for fault current analysis approach requires detailed and comprehensive over-current design and analyses.

## Liquid Nitrogen Losses in a Cooled HTS Coil

Coils fed from current source in every winding carries the same current. The magnetic field, however, varies both radially and axially over the coil. The axial field component is strongest inside of the coil and decreases linearly outwards due to change in sign just inside the outer surface of the coil. The radial field component is small in the middle of the coil, but increases towards the coil ends. Thus, this variation in amplitude and orientation of the magnetic field results in different operating conditions in different parts of the coil. Consequently, when employing anisotropic HTS tapes, such as BSCCO/Ag tapes, the AC losses vary greatly between different parts of a coil. Considering a large coil cooled by pool boiling liquid nitrogen at 77 K, a likely operating temperature for the HTS tape is around 80 K, taking the thermal resistance and the associated temperature drop between the winding and the liquid nitrogen into account. The maximum current in such a coil is limited by the highest magnetic field in the coil. Consider a coil where the highest field is 1 T. Then, from figure 1 it can be seen that by choosing a current less than the current yielding the AC loss minimum at 1T, that is, less than 52A, the entire coil will operate with unnecessarily high losses. When applying a current greater than 52A, the AC losses increase rapidly resulting in large losses in the high field part of the coil. These losses will not be compensated for by lower losses in other low field parts of the coil. Using figure 1 the optimum operating current can be determined for different magnetic fields at 80 K. For stability reasons (discussed below), a somewhat lower current than the value given by the lowest losses is probably preferable. In figure 2 the current is set to 44 A and then the AC losses in different parts of the coil can be determined depending on the temperature distribution in the coil. The temperature distribution depends on the heat generation, the cooling, and the heat transfer through the coil winding.

### Design Optimization of Coil

The magnetic field distribution in a coil is to a large extent given by the application. Furthermore, the current carried by the conductors in the coil is generally the same in the entire coil. Consequently, the parameter remaining for AC loss optimization in a coil is the temperature. With efficient cooling, i.e. low losses and low thermal resistance in the windings, the temperature may be kept almost uniform in the entire coil. The AC losses at various magnetic fields are then given by curve (a) in figure 2. For the efficiency of the coil this is unsatisfactory. The current is determined by the highest field of the coil (the field at the inner most winding of the coil). As the magnetic field decreases with increasing

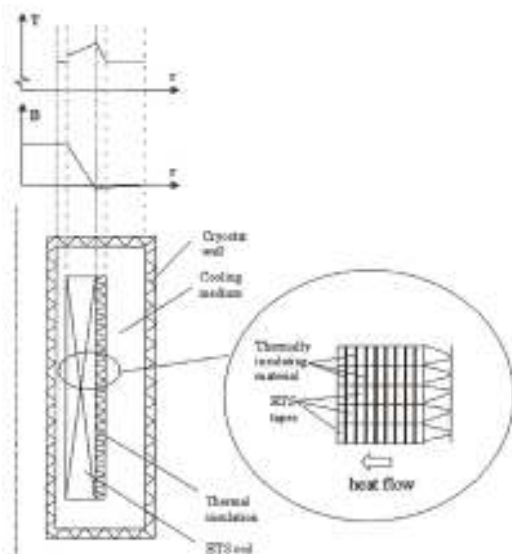


**Figure 3: Schematic overview of a coil with controlled heat flow.**

radius, the optimum operating temperature shifts to higher temperatures. Consequently, the HTS tape operates optimally only in the inner most winding. For large AC coils producing high magnetic fields, the

heat generation due to AC losses is considerable and a uniform temperature distribution is difficult to achieve. If the efficiency of the cooling is constant throughout the coil, the temperature becomes highest where the magnetic field is highest and the most power is dissipated. This corresponds to curve (b) in figure 2. The AC losses in this case become larger than for the case with a constant temperature in the coil. The optimum temperature/field combination is that indicated by curve (c) in figure 2. Here the operating temperature is close to the optimum temperature for every magnetic field. A coil with a corresponding temperature distribution operates optimally in every part of the coil with regard to the AC losses. This desired temperature distribution can be achieved by controlling the heat-flow through the winding. For instance, the heat generated in the coil can be forced to flow through the coil winding and exit only through the inner surface of the coil by applying thermal insulation on the outside of the coil, see figure 3. A temperature gradient with the highest temperature in the outer part of the coil where the magnetic field is the lowest is then established. To further adjust the temperature, thermally insulating materials can be inserted between layers of the HTS tape to increase the temperature gradient. Also considering perpendicular fields, an axial thermal gradient in addition to the radial gradient would be beneficial at the coil ends. Similar to the case with parallel magnetic field, the optimum operating temperature decreases with the field angle (the perpendicular field component) relative to the coil axis. The temperature should therefore be kept lower at the coil ends than in the middle of the coil.

### **HTS AC Analysis**

In the design of HTS AC components, knowledge about the optimum operating current, with respect to AC losses, is of great importance. Although related to  $I_c(T, B)$ , the optimum operating current can deviate significantly from this value. For instance, at 1 T and 80 K, the optimum current for the considered tape is 44 A (taking the stability margin into account), while  $I_c$  is only 31 A. By choosing  $I_c = 31$  A as the operating current, the AC losses become about 30% higher and about 40% more tape is required than when operating at the optimum current rating of 44 A. In this paper we propose to make the HTS tape to operate with a current close to the optimum current in every part of the coil by controlling the temperature in a coil. Alternative methods to achieve such a current would be to use different numbers of parallel tapes or tapes with different dimensions or quality in different parts of the coil. Then the current or the critical current of the tapes can be varied step-wise. Such solutions may be feasible. However, as this will require a large number of joints inside the coil, there are obvious disadvantages associated with such approaches. The hysteresis losses are customarily and also in the present paper modelled by assuming a magnetic field independent critical current, which is set equal to the self field critical current. However, one should note that at high magnetic fields the decrease in critical current is substantial and the actual hysteresis losses become somewhat lower than predicted by this model. This is mainly due to the lower screening currents that are set up inside the HTS tape as the critical current decreases with increasing magnetic field. If the field dependency is taken into account, the total losses become lower and the benefit from applying an optimum temperature distribution somewhat greater than shown in figure 4. Reduction of AC losses is crucial for AC HTS applications to become economically feasible. Any reduction of the AC losses in HTS power components results in lower energy costs as well as lower investment costs for the cooling machine. Major reduction of AC losses can be obtained through tape design, and this is an issue to be addressed by the tape manufacturers. However, the HTS component design itself will play an increasingly important role as the HTS tape performance is improved. Optimum thermal design of a coil as discussed in this paper is among the issues that provide significant benefits.

### **Modeling of Over Current and Analysis**

The over-current analysis consists of two parts. One is a system study that includes the electromagnetic behavior of the generator connected to an electrical grid through a step up transformer and mechanically coupled to a turbine. The other is a detailed thermal model of the coil to analyze the coil response to the current and the field during the fault.

#### **A. System Model**

The fault currents are computed using a system model with a two-dimensional (2-D) finite-element electromagnetic model of the generator coupled to an external mechanical and electrical circuit in Flux

2D, a commercial FE package. The system is illustrated in Fig. 4. Inputs to the model are the turbine power characteristic, moment of inertia, generator EM design, transformer reactance, load characteristic (stiff voltage source or isolated load impedance), and exciter control logic. The key outputs are terminal voltage, armature currents, field current/voltage, generator speed, generator angle, mechanical power, electrical power, and reactive power. The model is first run under steady-state full-load conditions for 3 s until all voltages and current stabilize. The short circuit switches are then suddenly closed and reopened after 18 electrical cycles. The field coil is driven by a constant dc voltage of 2 V throughout the simulation. The system parameters employed in the model are the following:

- transformer reactance pu;
- end reactance pu;
- grid Thevenin voltage kV;
- grid Thevenin impedance pu.

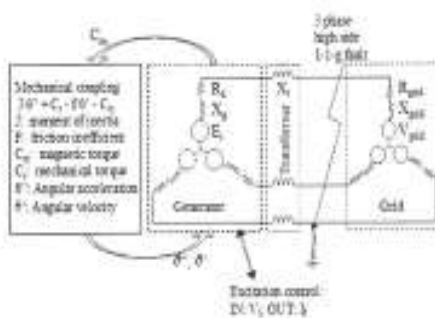


**Figure 4: System model for fault current analysis**

The bulk of field current during the transient is induced in the coil. The action of an automatic voltage regulator and exciter affects the outcome by only a few percent. The field current during the fault is a direct result of the armature current transient and the flux conditions in the machine. The DC transient in the field coil is induced by large three-phase currents in the armature during the fault. The 60 Hz ac portion visible in the field current is induced as a response to the dc offsets presenting in the armature fault current. At the end of the fault, the generator has accelerated ahead of the power system and has experienced a drop in terminal voltage. At this point, the generator is reconnected to the line and must come back into step with the power system. The generator acts as a torque source (i.e., motor) to pull the prime mover back into phase with the power system. There is also an armature current surge as a result of the voltage difference between the generator and the power system. The armature current surge induces a component of field current as the voltage recovers. The combination of phase and voltage recovery cause the large current overshoot seen after the fault is cleared from the line. The field current rises to about 160 A during the fault and reaches a peak of 180 A during the recovery. Peak fields of 2.6 T are obtained during this period.

### **B. Coil Thermal Model**

The thermal conductivity in the transverse direction is about an order of magnitude higher than that in the radial direction. The initial coil temperature distribution is calculated under the normal operation heat loads: the radiation and conduction heat and the Joule heating of the splice joints. Helium gas warms up from its inlet temperature and reaches its highest temperature near the exit. Consequently, the coil temperature near the helium exit point has the highest temperature and is used as the initial temperature of the coil in the over-current analysis. During an over-current fault, the current and the magnetic field of the field coil far exceed its normal operation values and the conductor becomes normal for a short period of time. The Joule heating of the HTS conductor per unit length is

$$g = \begin{cases} \min \left[ I_F (I_F - I_C) \frac{\rho_s}{A_s}, I_F \alpha I \left( \frac{I_F}{I_C} \right)^n \right] & T \leq T_C \\ I_F^2 \frac{\rho_e}{A} & T > T_C \end{cases} \quad (1)$$

where  $I_F$  = Field current;  $\rho_s$  = HTS tape residual resistivity;  $\rho_e$  = total conductor resistivity;  $A$  = total conductor cross-sectional area;  $A_s$  = HTS cross section;  $\alpha$  = 100 $\mu$ V/m;  $n$ = number between 11 and 15;  $T_C$  = HTS tape transition temperature;  $I_C$  = critical current, which is a strong function of magnetic field and temperature. This case the base field current ( $A$ ) is different from that listed in Table I. This is because during the analysis, we kept increasing the baseline of the field current until we saw substantial resistive heating. After the fault is cleared, the coil remains superconducting and fully functional. The small temperature rise for this case does not indicate too much design margin in the coil, however.

## Conclusion

Optimum current in terms of the AC losses in an HTS tape depends on the temperature and the magnetic field in which the tape operates. In a coil, the current is normally constant, while the magnetic field decreases with the radius. In large HTS AC coils the temperature may easily become highest in the region with the highest magnetic field since the AC losses are greatest in this part of the coil. Such a temperature distribution is very unfavourable as it further increases the losses. By introducing a controlled heat-flow in the coil, the temperature distribution can be adjusted such that an increase in the temperature compensates for a reduction in the magnetic field. Calculations for a commercial BSCCO/Ag HTS tape indicate that in coils with a maximum peak magnetic field above 0.5 T, the potential for loss reduction is about 10% when an optimum temperature distribution in the coil is attained.

Approach for designing HTS coils with sufficient margin to ride through transient over-currents has been developed. Evaluation of the coil over-current capability requires a detailed quench model with all system interactions and nonlinear properties, as described above. The analysis illustrates the challenge of coil quench protection during a fault. When the temperature is low and the current exceeds the coil by a small amount, the coil temperature rises slowly. The rate of temperature rise accelerates quickly as the current exceeds further. Eventually, as coil current and temperature rises further, the of the HTS conductor itself is exceeded everywhere and the coil becomes fully normal. Then the coil temperature rises rapidly, as fast as 200 K/s, due to the high fault current and low current-carrying capacity of HTS tape in its normal state.

## References

- [1] J Kellers, "Reliable commercial HTS wire for power applications" Presented at *EUCAS Copenhagen, 26–30 August 2001*
- [2] Z Han, P Boden, W G Wang, M D Bentzon, Skov-Hansen P, Goul J, Vase P 1999 *IEEE Trans. Appl. Supercond.* **9** 2537–40, 2001
- [3] N J Kelley, C Wakefield, M Nassi, P Corsaro, S Spreafico, D W Von Dollen, J Jipping, *IEEE Trans. Appl. Supercond.* **11** 2461–6
- [4] Stovall J P, Demko J A, Fisher P W, Gouge M J, Lue J W, Sinha U K, Armstrong J W, Hughey R L, Lindsay D and Tolbert J C 2001 *IEEE Trans. Appl. Supercond.* **11** 2467–72
- [5] Will'en D "Installation and operation of a 2 kA(rms) HTS power cable in a public utility grid" Presented at *EUCAS Copenhagen, 26–30 Aug. 2001*
- [6] Therond P H, Levillain C, Picard J F, Bugnon B, Zeuger H, Hornfeldt S, Fogelberg T, Papst G and Bonmann D 1998 *Cigre 37th Session Paper 12-302 (30 Aug.–5 Sept. 1998)*

- [7] Runde M and Magnusson N 2001 Induction heating of aluminium billets using superconducting coils 2002 *Physica C* at press
- [8] Magnusson N and Hornfeldt S 1998 *Rev. Sci. Instrum.* **69** 3320–5
- [9] Magnusson N, Schönborg N, Wolfbrandt A and Hornfeldt S 2001 *Physica C* **354** 197–201
- [10] Rabbers J J, ten Haken B and ten Kate H H J 2001 *Rev. Sci. Instrum.* **72** 2365–73
- [11] Ashworth S P and Suenaga M 2001 *Cryogenics* **41** 77–89
- [12] Bean C P 1964 *Rev. Mod. Phys.* **36** 31–9
- [13] Ashworth S P and Suenaga M 2000 *Physica C* **329** 149–59
- [14] Magnusson N 2001 *Physica C* **349** 225–34
- [15] Wolfbrandt A, Magnusson N and Hornfeldt S 2001 Temperature dependence of AC losses in a BSCCO/Ag tape exposed to AC magnetic fields in different orientations 2002 *Physica C* at press
- [16] ten Haken B, Rabbers J J and ten Kate H H J 2002 *Physica C* at press
- [17] Al-Mosawi M K, Beduz C, Yang Y, Webb M and Power A 2001 *IEEE Trans. Appl. Supercond.* **11** 2800–3
- [18] Godeke A, Shevchenko O A, Rabbers J J, ten Haken B, Spoorenberg C J G, Klein Schiphorst P, Damstra G C and ten Kate H H J 2001 *IEEE Trans. Appl. Supercond.* **11** 1570–3
- [19] Carr W J 1979 *IEEE Trans. Magn.* **15** 240–3
- [20] Magnusson N and Hornfeldt S 1999 *IEEE Trans. Appl. Supercond.* **9** 785–8
- [21] Norris W T 1970 *J. Phys. D: Appl. Phys.* **3** 489–507
- [22] J. W. Lue, M. S. Lubell, D. Aized, J. M. Campbell, and R. E. Schwall, “Spontaneous quenches of a high temperature superconducting pancake coil,” *IEEE Trans. Magn.*, vol. 32, no. 4, pp. 2613–2616, Jul. 1996.
- [23] O. Tsukamoto, J. Chen, and S. Akita, “Stability characteristics of fully superconducting and damperless generator connected to power grid,” *IEEE Trans. Appl. Supercond.*, vol. 3, no. 1, pp. 377–380, Mar. 1993.
- [23] J. L. Smith, J. L. Kirtley, S. Sunder, and S. Umans, “Performance of MIT 10MVA superconducting generator rotor,” *IEEE Trans. Appl. Supercond.*, vol. 5, no. 2, pp. 445–448, Jun. 1995.
- [25] *American National Standard Requirements for Synchronous Machines*, ANSI C50.
- [26] E. Vassent, G. Meunier, A. Foggia, and G. Reyne, “Simulation of induction machine operation using a step by step finite element method coupled with circuits and mechanical equations,” *IEEE Trans. Magn.*, vol. 27, no. 11, pp. 5232–5234, Nov. 1991.